

@p@12.5

12.5th International Workshop on Positron and Positronium Chemistry
September 2, 2021, Online

Dissolved oxygen sensing by positronium for PET

Kengo Shibuya*, H. Saito
Univ. of Tokyo, Japan

F. Nishikido, M. Takahashi, T. Yamaya
NIRS-QST, Japan



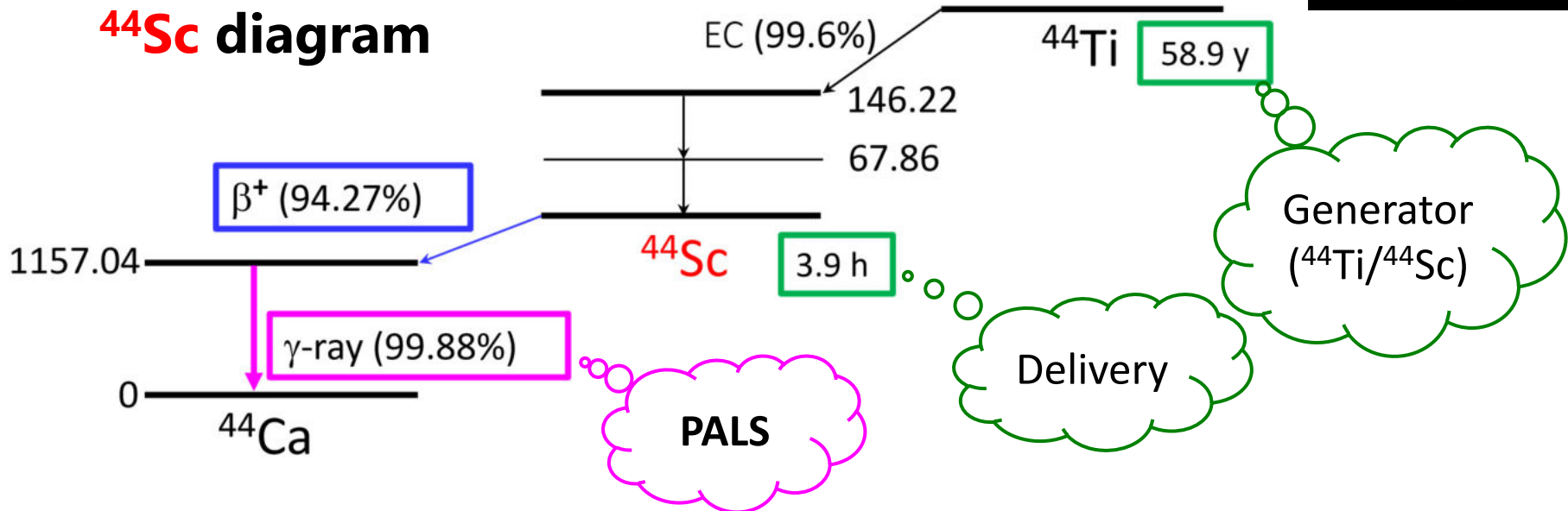
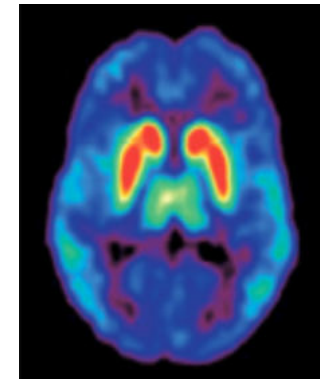
Positron Emitters in PET

■ Conventional PET isotopes: ^{11}C , ^{13}N , ^{15}O , ^{18}F

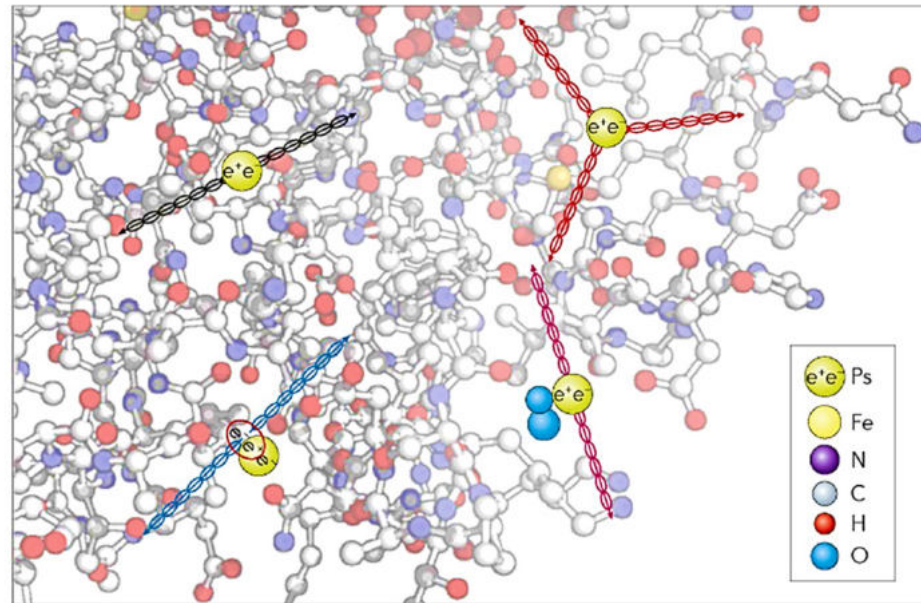
■ Advanced PET isotopes: ^{44}Sc , ^{64}Cu , ^{76}Br , ^{89}Zr , ^{90}Y , ^{124}I , etc.

aiming for

- new tracer
- multi-modal imaging (PET/MRI, PET/SPECT, ...)
- radio-theranostics (nuclear imaging + radio-therapy)



Positronium Lifetime Imaging (PALS/PET)



[1] P. Moskal *et al*, *Nature Rev. Phys.* **1** (2019) 527.

[2] P. Moskal *et al*, *EJNMMI Phys.* **7** (2020) 44.

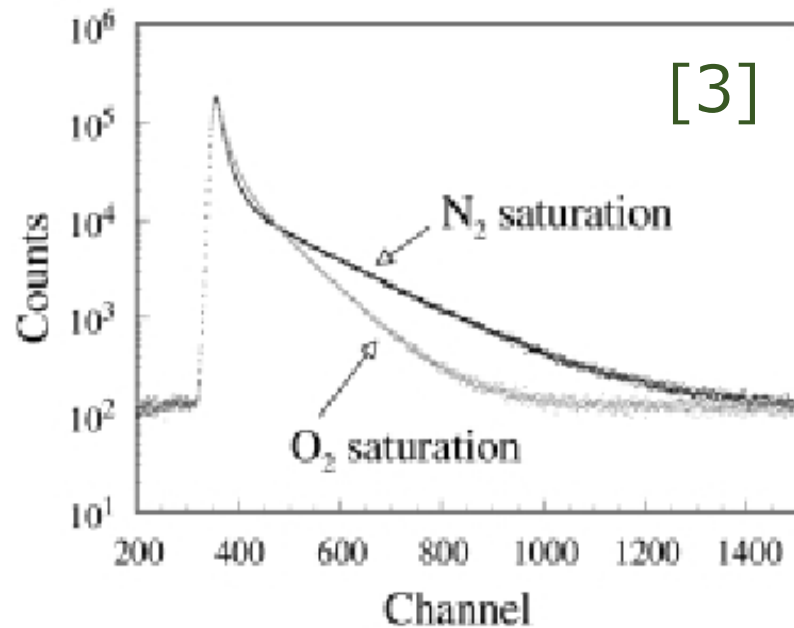
Around 30% positron annihilates after forming Ps *in vivo*, and the lifetime depends on

- free volume
 - oxygen [This talk.]
 - bio-active molecules (radicals)
- ... possibility as biomarker.

o-Ps Quenching paths

1. Pick-off
2. Electron exchange (unpaired electron)
3. Chemical bonding/trapping (PsO_2)
4. ~~Spin conversion (spin-orbit)~~

Liquid experiments must remove O_2 gas by bubbling / freeze-pump-thaw.



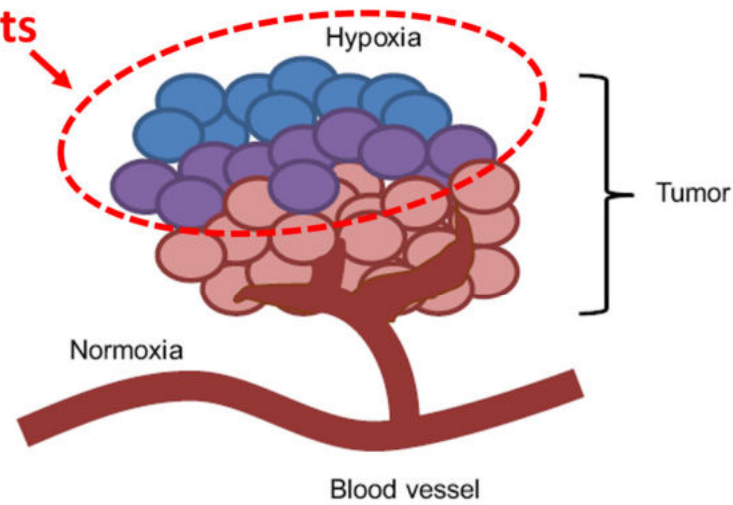
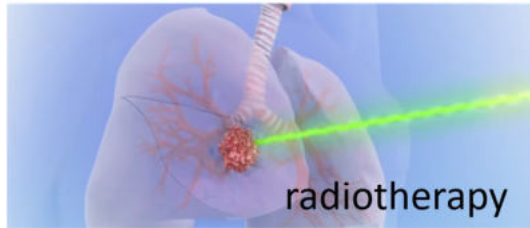
↓

Ps may be used for an O_2 sensor.

[3] Y. Kino *et al*, *J. Nucl. Radiochem. Sci.* **1**, 63 (2000) 63.

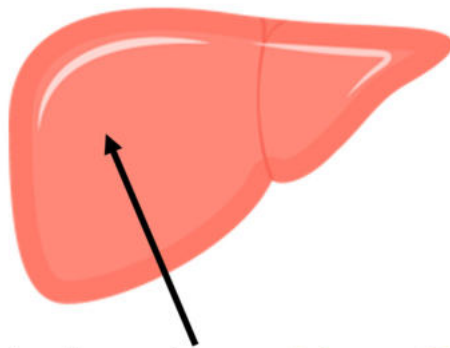
Motivation: hypoxia sensing

resistant to treatments

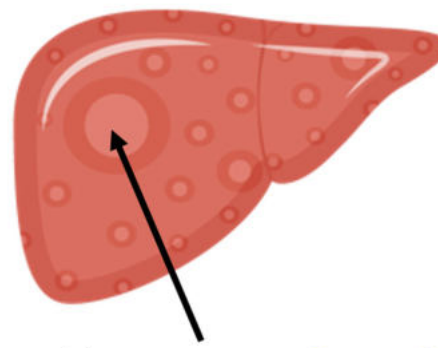


[4] K. Graham, *Int. J. Nanomed.* **13** (2018) 6049.

pO₂ in Liver



Healthy liver tissue: **41 mmHg**

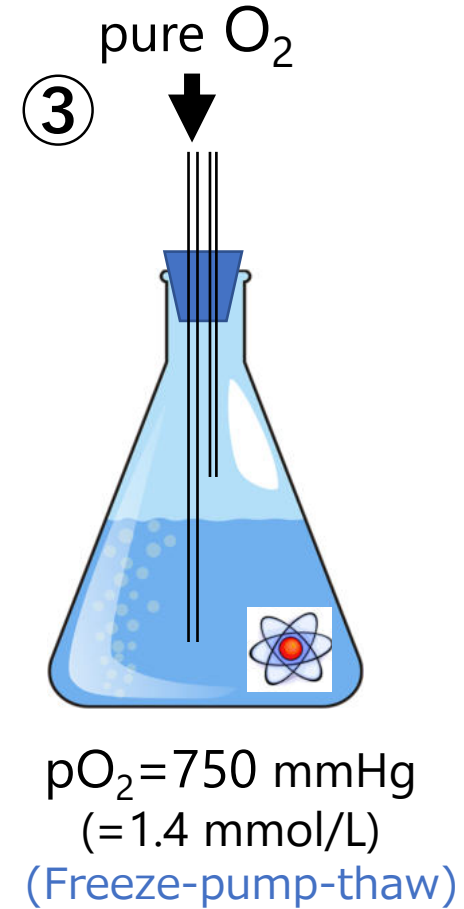
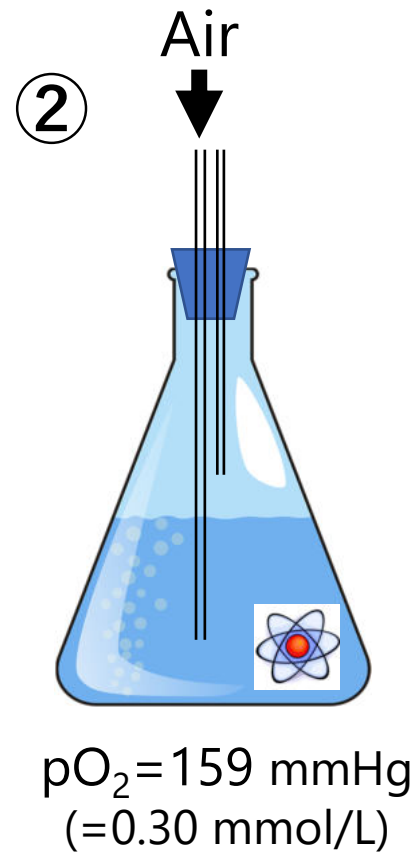
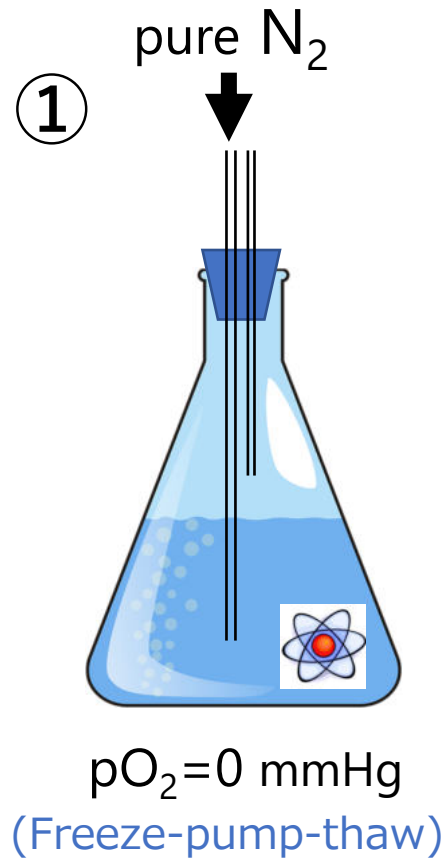


Liver tumor: **6 mmHg**

[5] A. Carreau, *J Cell Mol Med.* **15** (2011) 1239. [6] P. Vaupel, *Antioxid Redox Signal* **9** (2007) 1221.

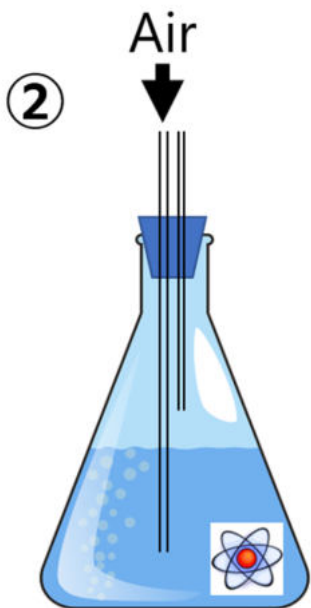
Measurements and Results

Samples

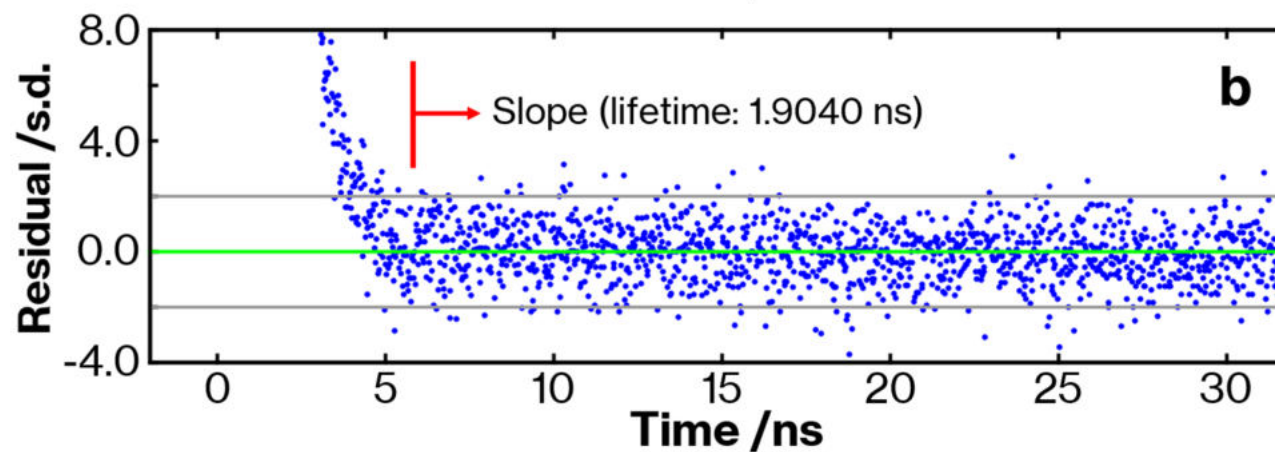
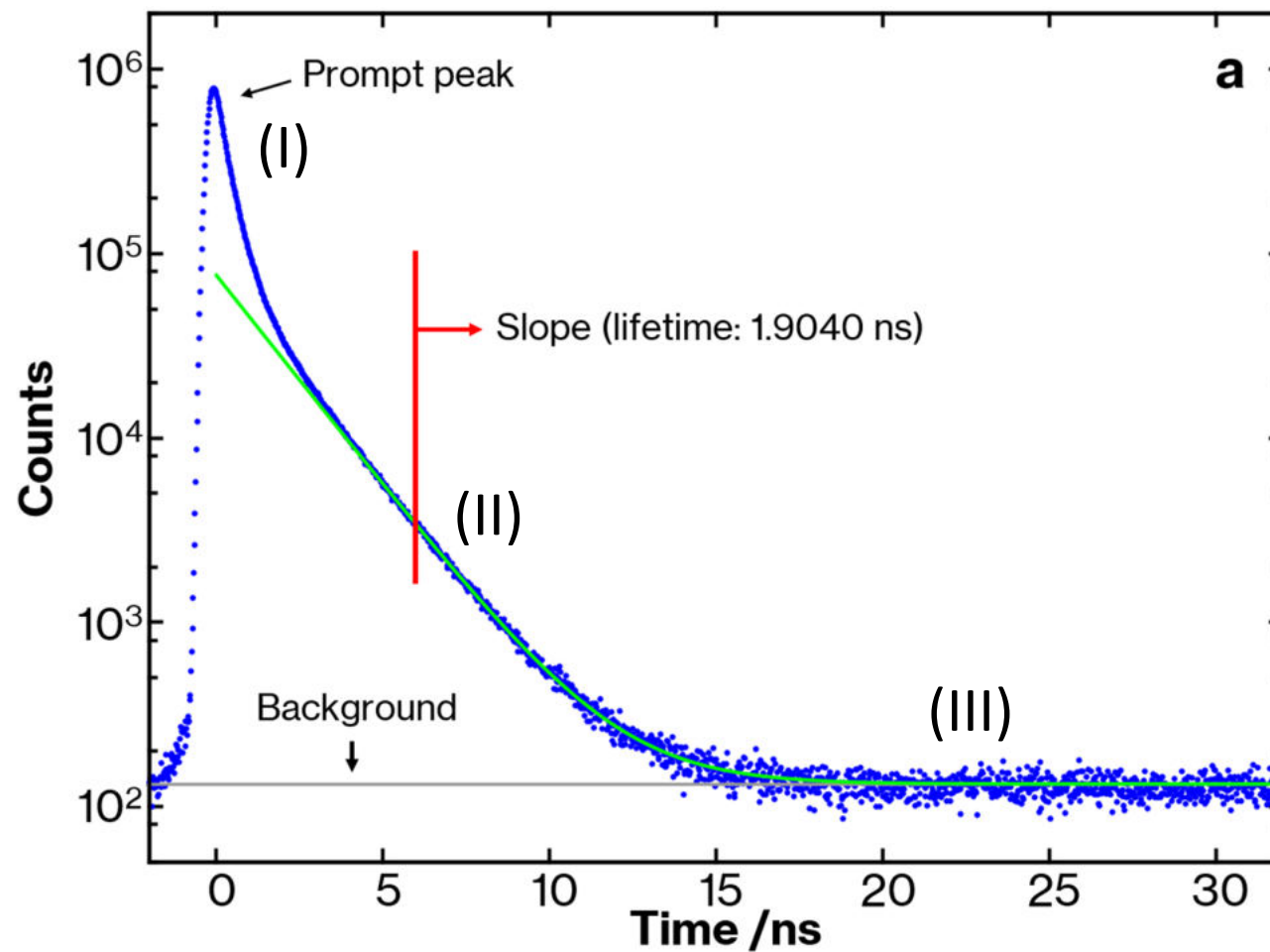


²²NaCl : positron emitter
200 kBq

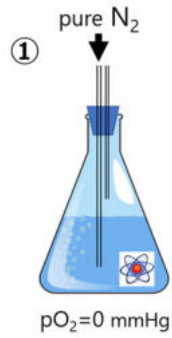
Data (Air-saturated)



$pO_2 = 159$ mmHg

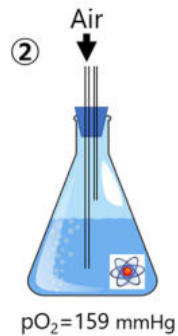


Results



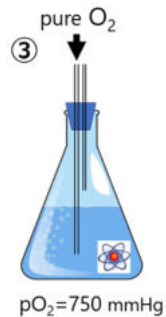
$$\tau_{\text{N}_2} = 1.9215(32) \text{ ns}$$

$$\Rightarrow \lambda_{\text{o-PS}} + \lambda_{\text{H}_2\text{O}} + 705.1(7) \kappa_{\text{N}_2} = \frac{1}{\tau_{\text{N}_2}} = 548.3(1.1) \mu\text{s}^{-1}$$



$$\tau_{\text{Air}} = 1.9040(29) \text{ ns}$$

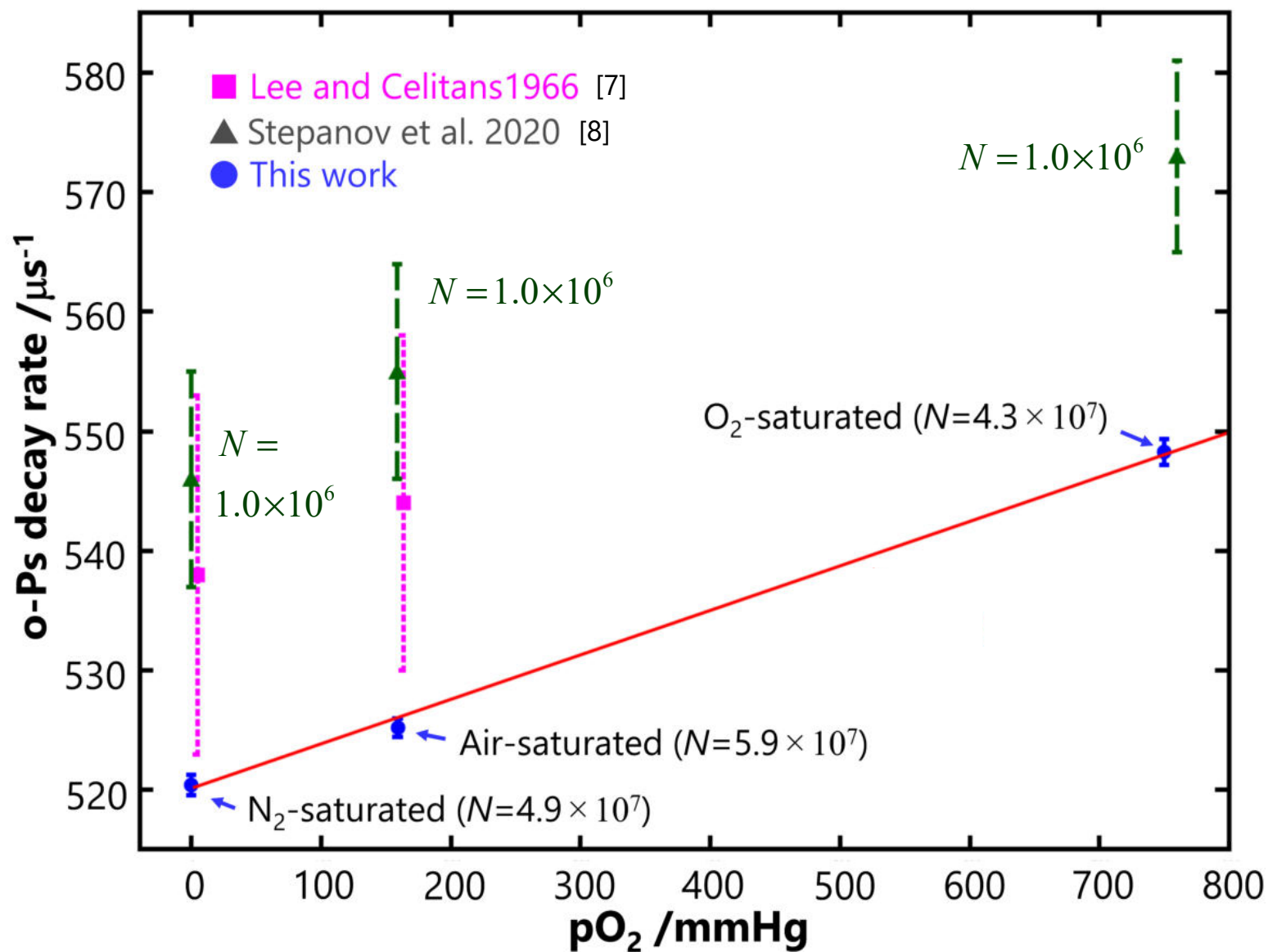
$$\Rightarrow \lambda_{\text{o-PS}} + \lambda_{\text{H}_2\text{O}} + 296.0(3) \kappa_{\text{O}_2} + 556.1(5) \kappa_{\text{N}_2} = \frac{1}{\tau_{\text{Air}}} = 525.2(8) \mu\text{s}^{-1}$$



$$\tau_{\text{O}_2} = 1.8239(36)$$

$$\Rightarrow \lambda_{\text{o-PS}} + \lambda_{\text{H}_2\text{O}} + 705.1(7) \kappa_{\text{O}_2} = \frac{1}{\tau_{\text{O}_2}} = 548.3(1.1) \mu\text{s}^{-1}$$

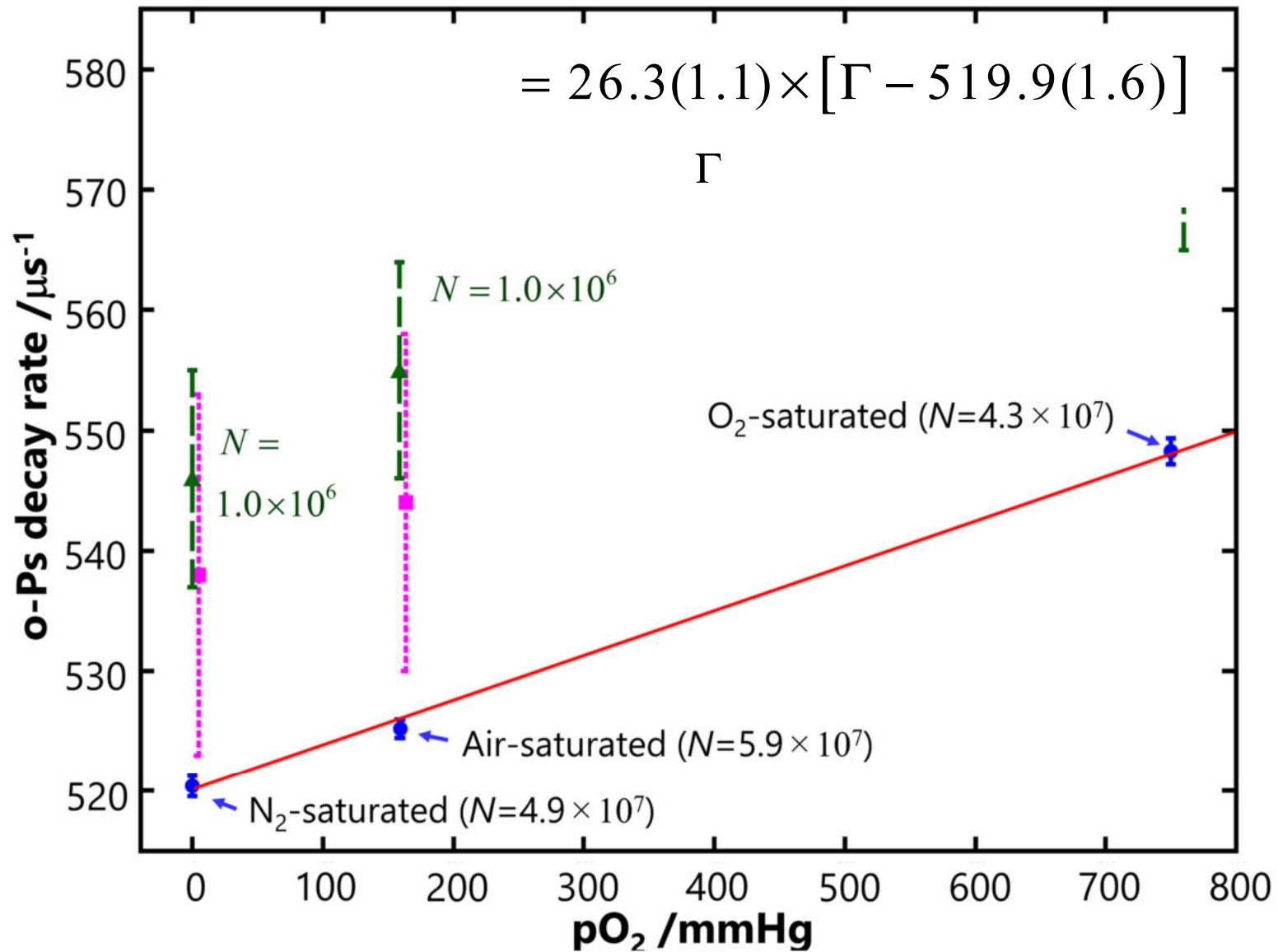
pO₂ vs o-Ps Decay rate



[7] J. Lee & G. J. Celitans, *J. Chem. Phys.* **44** (1966) 2506.

[8] P. S. Stepanov et al., *Phys. Chem. Chem. Phys.* **22** (2020) 5123.

pO_2 vs *o*-Ps Decay rate

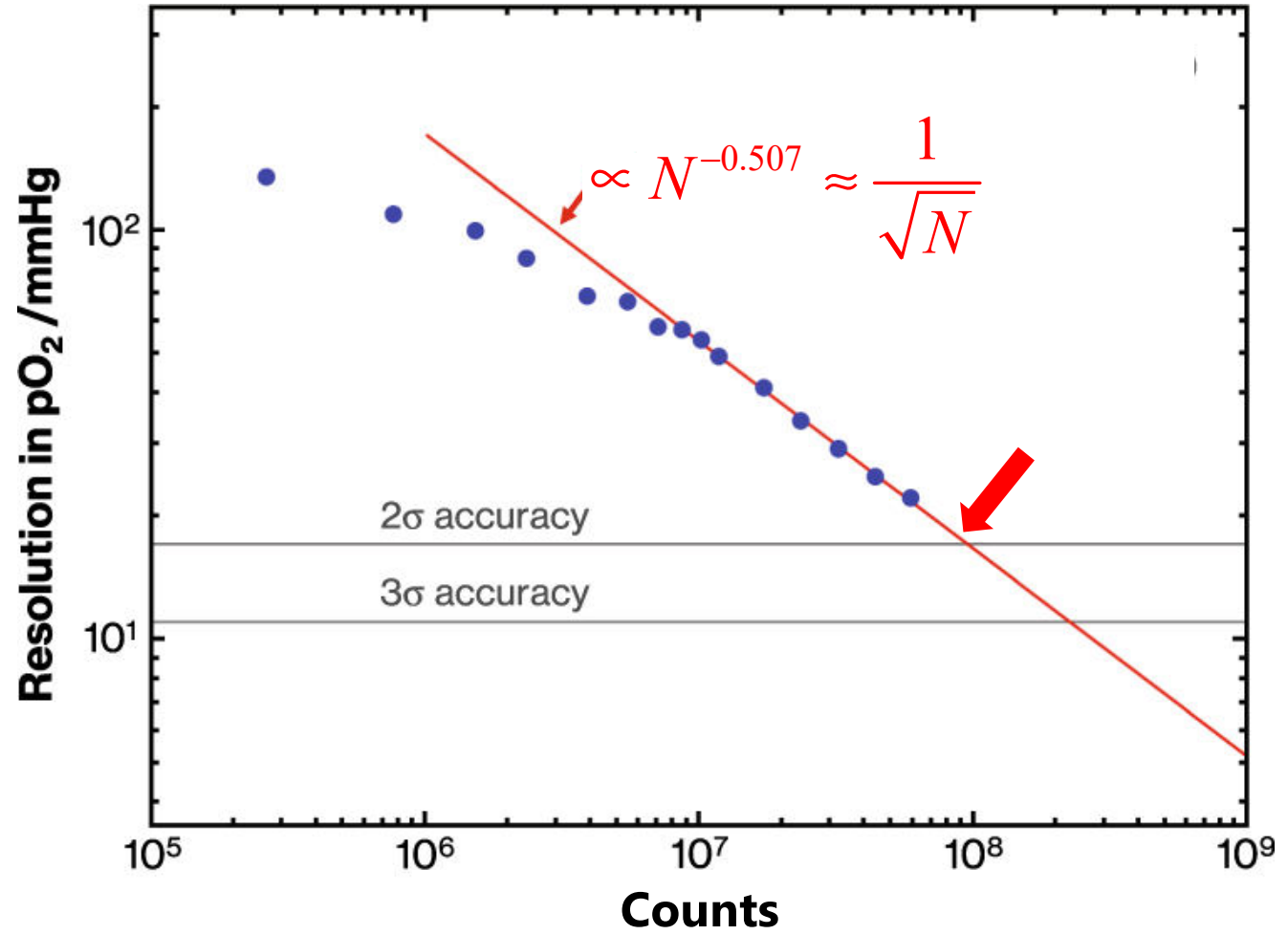
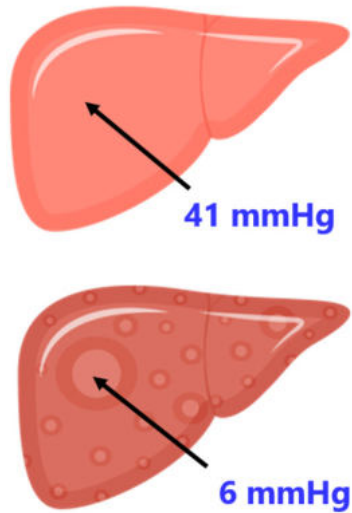


[7] J. Lee & G. J. Celitans, *J. Chem. Phys.* **44** (1966) 2506.

[8] P. S. Stepanov et al., *Phys. Chem. Chem. Phys.* **22** (2020) 5123.

Counts vs pO₂ Resolution

Resolution



Discussion

10^8 counts possible?

↑ Activity

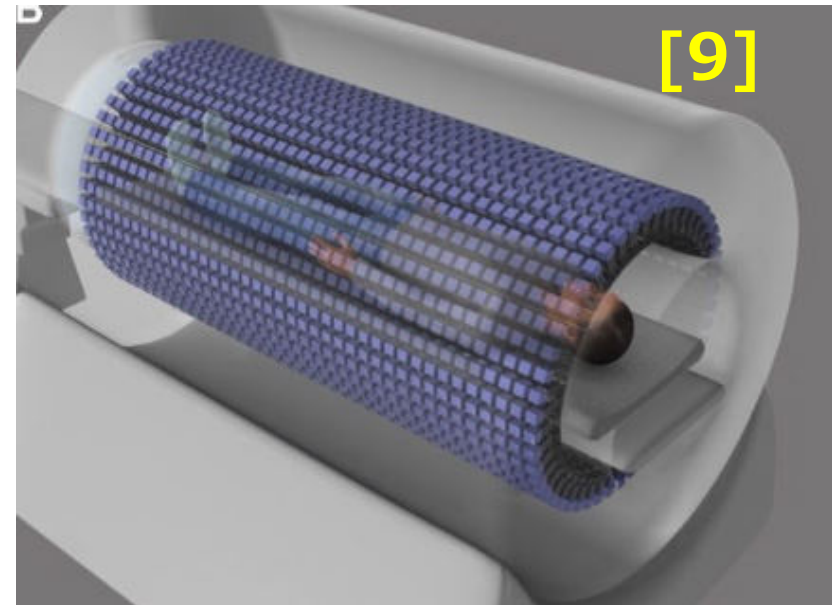
- this measurement: 200 kBq
- **FDG-PET scan: 200 MBq**

↑ Solid angle

- this: ca 5%
- **whole-body scanner: >60%**

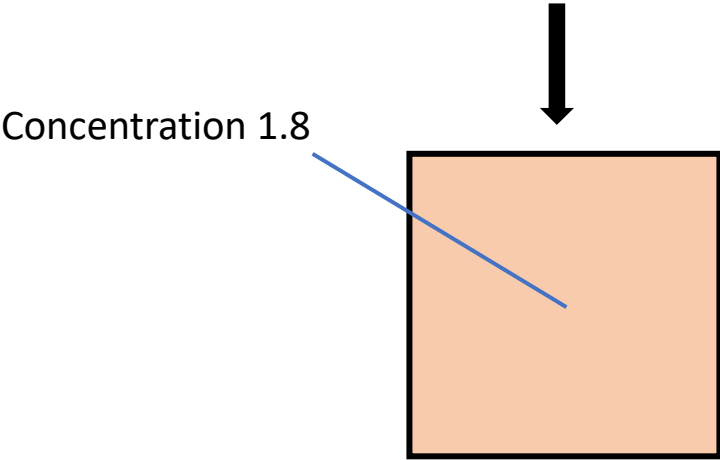
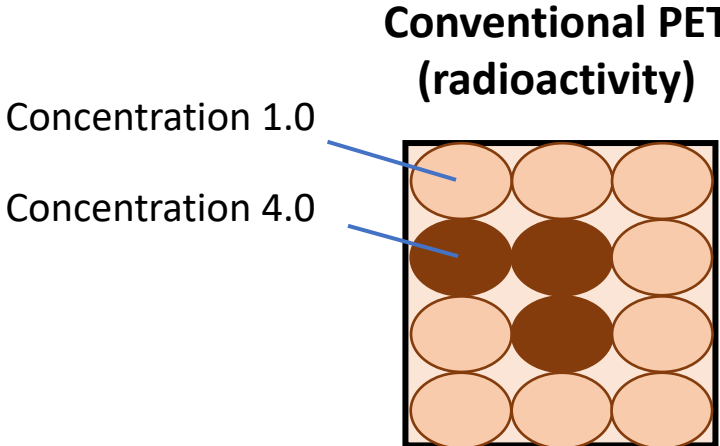
↓ Triple coincidence required

↓ Within 30 min

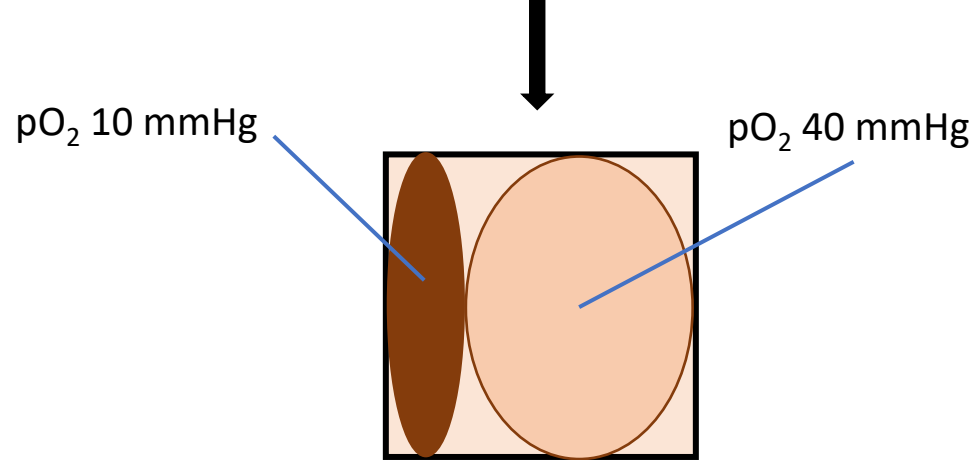
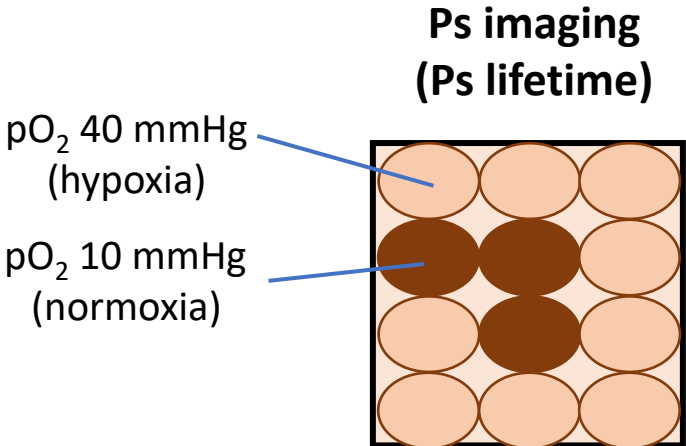


[9] S. R. Cherry, et al. *J. Nucl. Med.* vol. **59**, pp. 3–12 (2018).

Larger voxel available



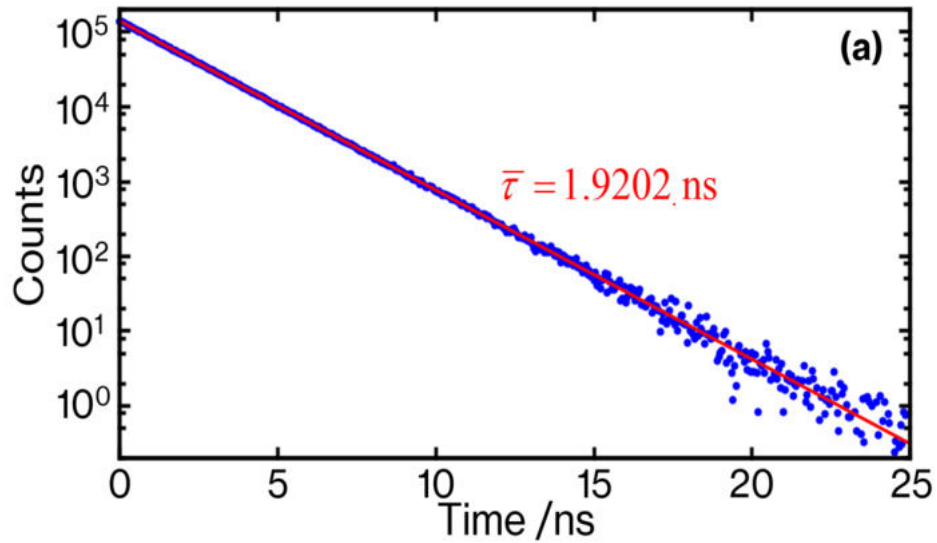
The interior of the voxel is assumed to be uniform, and no information other than the averaged concentration is outputted.



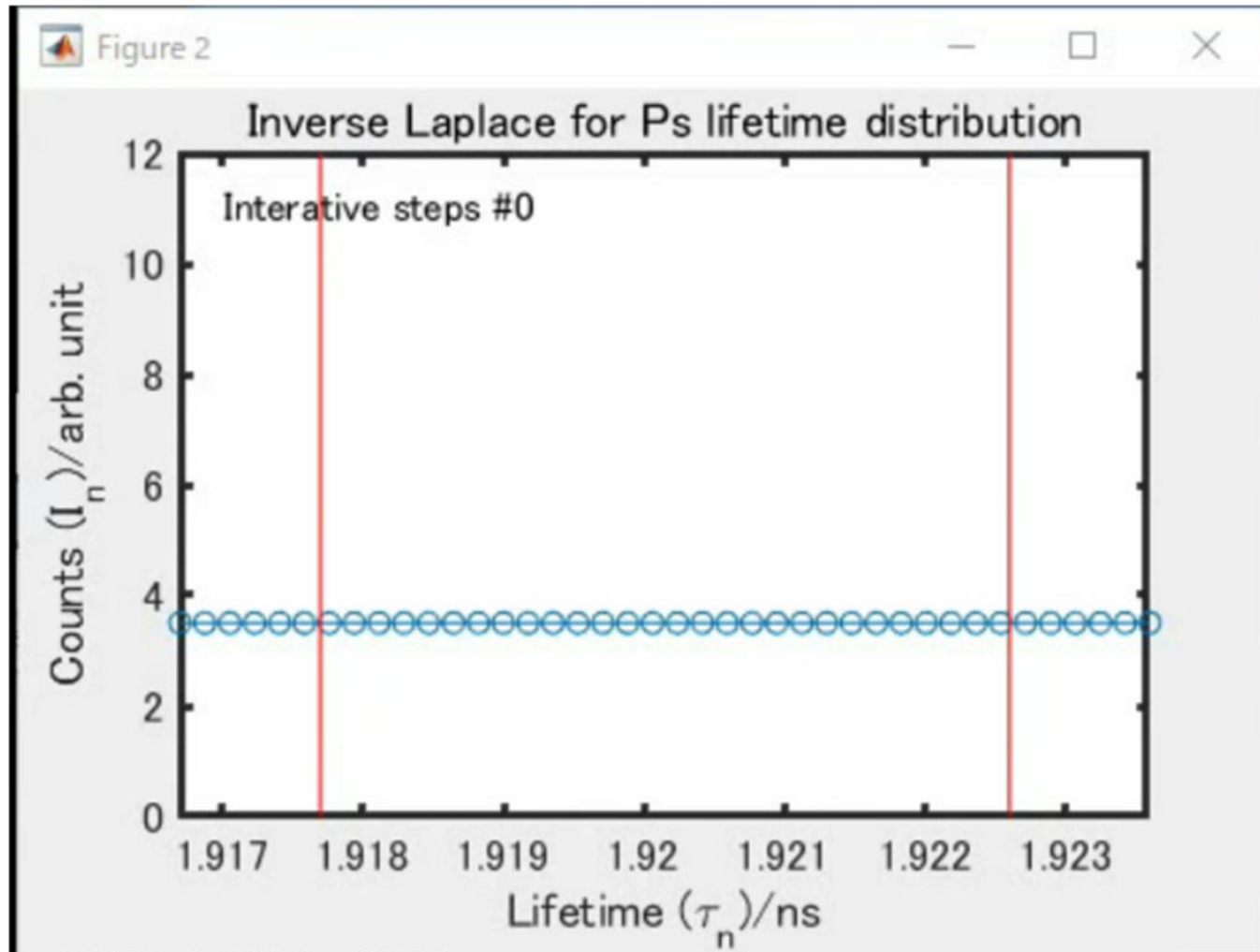
The lifetime components are separatable to output the lifetime and the amount of each component.

Inverse Laplace transform (CONTIN^[10])

$$\begin{cases} F(t) = \exp(-\lambda t) \\ f(x) = \mathcal{L}^{-1}\{F(t)\} = \delta(x - \lambda) \end{cases}$$



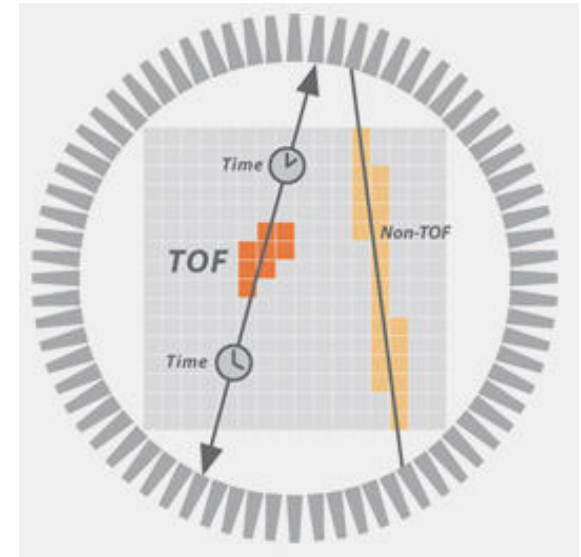
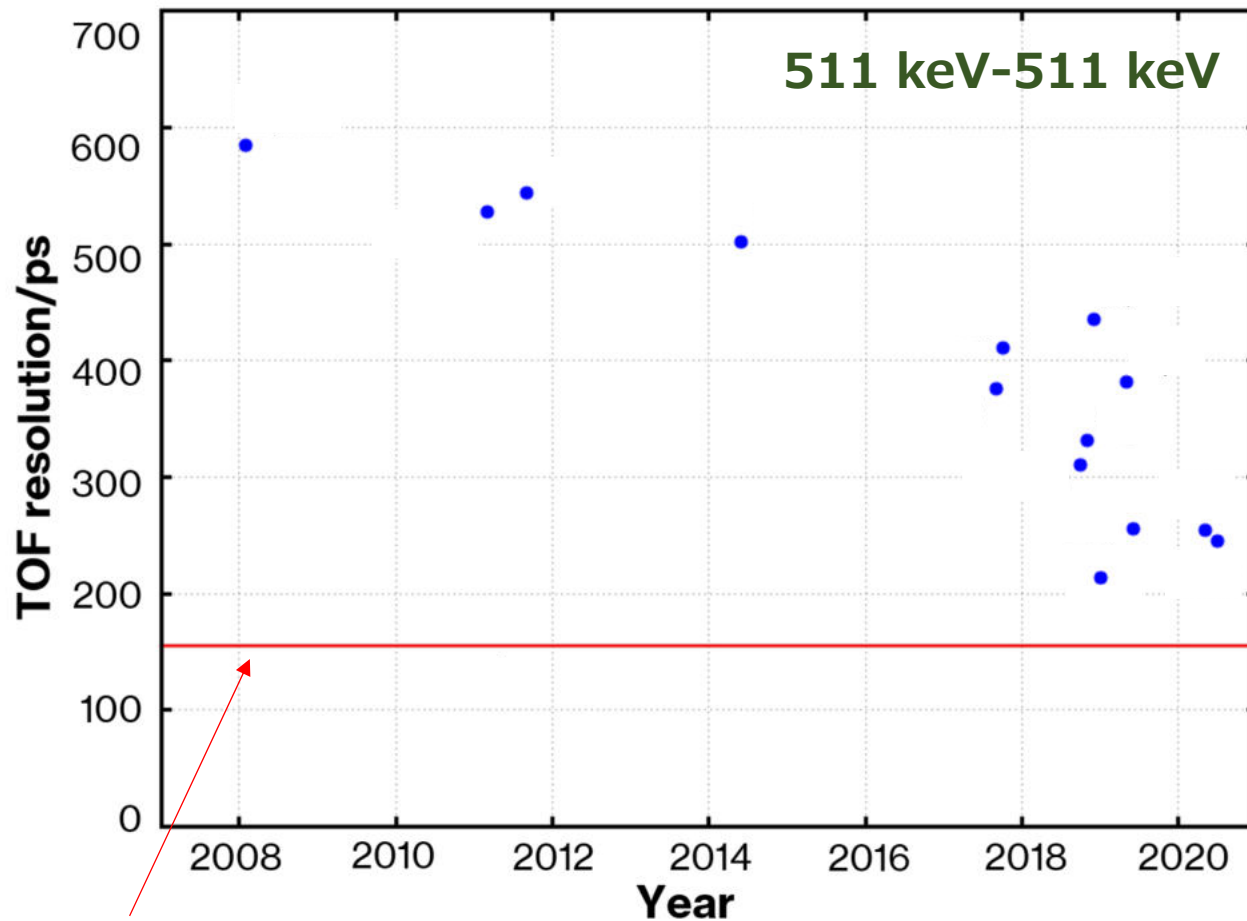
CONTIN (Video)



Evaluation function

$$\begin{aligned}
 & \text{system matrix} & \text{solution} & \text{data} \\
 J_0 \equiv & \begin{pmatrix} \exp\left(-\frac{t_1}{\tau_1}\right) & \exp\left(-\frac{t_1}{\tau_2}\right) & \dots & \exp\left(-\frac{t_1}{\tau_n}\right) \\ \exp\left(-\frac{t_2}{\tau_1}\right) & \exp\left(-\frac{t_2}{\tau_2}\right) & \dots & \exp\left(-\frac{t_2}{\tau_n}\right) \\ \exp\left(-\frac{t_3}{\tau_1}\right) & \exp\left(-\frac{t_3}{\tau_2}\right) & \dots & \exp\left(-\frac{t_3}{\tau_n}\right) \\ \vdots & \vdots & \ddots & \vdots \\ \exp\left(-\frac{t_m}{\tau_1}\right) & \exp\left(-\frac{t_m}{\tau_2}\right) & \dots & \exp\left(-\frac{t_m}{\tau_n}\right) \end{pmatrix} & \begin{pmatrix} \frac{I_1}{\tau_1} \\ \frac{I_2}{\tau_2} \\ \frac{I_3}{\tau_3} \\ \vdots \\ \frac{I_n}{\tau_n} \end{pmatrix} & \begin{pmatrix} S_n(t_1) - B \\ S_n(t_2) - B \\ S_n(t_3) - B \\ \vdots \\ S_n(t_m) - B \end{pmatrix} \\
 & & & \left. \vphantom{\begin{pmatrix} S_n(t_1) - B \\ S_n(t_2) - B \\ S_n(t_3) - B \\ \vdots \\ S_n(t_m) - B \end{pmatrix}} \right|^2 \\
 & & & + \alpha^2 \left[\left(\frac{I_1}{\tau_1}\right)^2 + \left(\frac{I_2}{\tau_2}\right)^2 + \dots + \left(\frac{I_n}{\tau_n}\right)^2 \right] \\
 & & & \text{regularizer (general)} \\
 J_1 = \sum_{j=1}^m & \left\{ \frac{\left[\sum_{i=1}^n \frac{I_i}{\tau_i} \exp\left(-\frac{t_j}{\tau_i}\right) \right] - [S_n(t_j) - B]}{\sqrt{S_n(t_j)}}} \right\}^2 & + \alpha^2 \sum_{i=1}^{n-2} & \left(\frac{I_i}{\tau_i} - 2 \frac{I_{i+1}}{\tau_{i+1}} + \frac{I_{i+2}}{\tau_{i+2}} \right)^2 \\
 & & & \text{regularizer (CONTIN)}
 \end{aligned}$$

Timing resolution for lifetime spectroscopy



[11] H. Saito, et al, *Nucl. Instrum. Methods A* **vol. 487**, pp. 612–617 (2002).

Background (random coincidence)

high quality delay cable. For the direct and inverted spectra there is a loss of signal due to conversion of signal events into randoms, so that the *measured* spectrum for a single exponential signal with decay constant λ as a function of time t has the form

$$(A e^{\pm\lambda t} + B) e^{-nt} \quad (1)$$

where A and B are constants, n the stop rate and the positive sign for λ applies to the inverted spectrum. The usual approximation $e^{-nt} = 1$ is not sufficiently accurate when n is large.

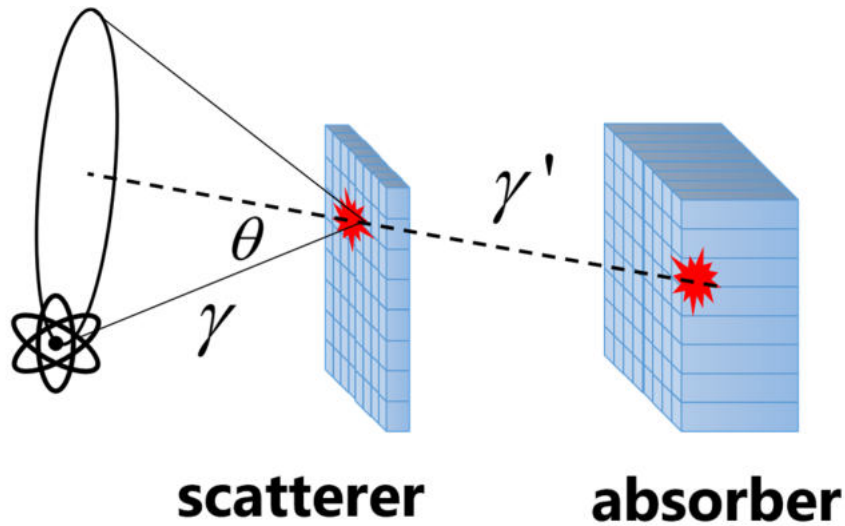
[12] P. G. Coleman *et. al*, *J. Phys. E*, **5** (1972) 376.

With the stop counting rate, η , the probability having no stop until time, t , and having the stop in the next Δt :

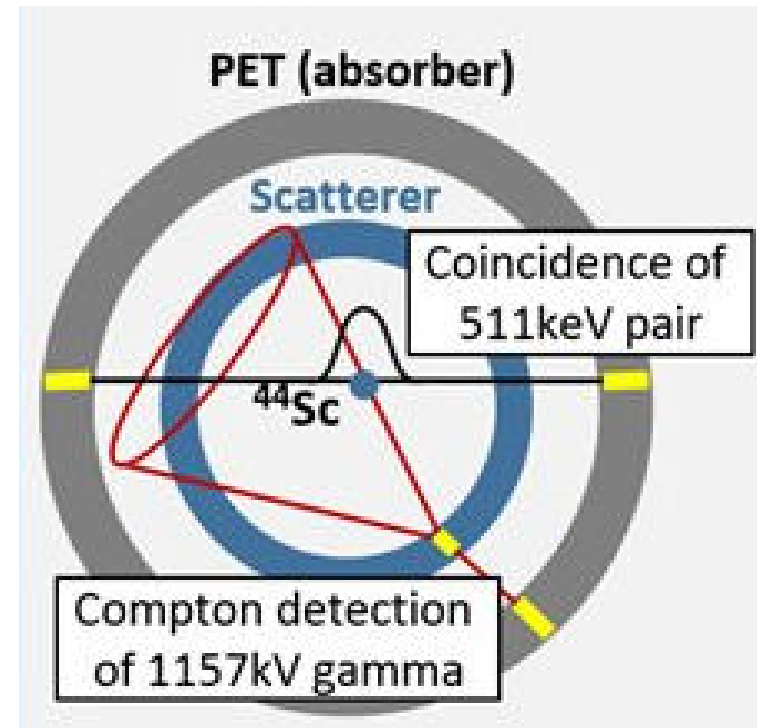
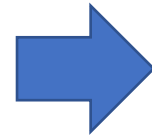
$$\lim_{\Delta t \rightarrow \infty} (1 - \eta \Delta t)^{\frac{t}{\Delta t}} \cdot \eta \Delta t \rightarrow C_1 \exp(-\eta t) \quad \because \lim_{n \rightarrow \infty} \left(1 + \frac{1}{n}\right)^n = e$$

Compton camera technique

Compton camera



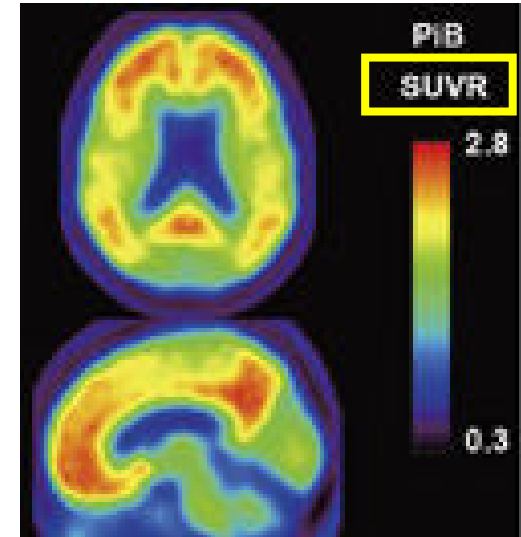
$$\theta = \cos^{-1} \left[1 + m_e c^2 \left(\frac{1}{E_\gamma} - \frac{1}{E_{\gamma'}} \right) \right]$$



[13] E. Yoshida, Phys. Med. Biol., vol. 65, pp. 125013 (2020).

Absoluteness (SUV vs mmHg)

- **SUV** (standardized uptake value) depending on
 - scanner
 - protocol
 - corrections
 - reconstruction algorithm
 - other situations.



SUV=1:

average radioactive concentration

GE Healthcare

- **pO₂ in mmHg**
 - enable comparison data between deferent protocols.

Summary

- A linearity between pO_2 and o-Ps decay rate was observed.
(proportionality: $26.3 \pm 1.1 \text{ mmHg}/\mu\text{s}^{-1}$)
- 100M counts provides pO_2 resolution of 17 mmHg which is enough to discriminate hypoxia from normoxia.
- An inverse Laplace transform may divide Ps lifetime components for a larger voxel in Ps imaging.
- We are planning to combine PET with Compton Camera technique for Ps lifetime imaging.

[12] K. Shibuya, *et al.*, *Commun. Phys.* **3**, 173 (2020).

[\[OPEN ACCESS\]](#)

Backup Slides

